12th International Conference on Hydroscience & Engineering
Hydro-Science & Engineering for Environmental Resilience
November 6-10, 2016, Tainan, Taiwan.

Development and Validations of a 3-D Numerical Wave Model in Cartesian Grid System Using Level Set Method

Yu-Chen Chang, Ching-Jer Huang, Chun-Yuan Lin
Department of Hydraulic and Ocean Engineering, National Cheng Kung University
Tainan, Taiwan

ABSTRACT

A three-dimensional (3-D) numerical wave model based on a multi-block Cartesian grid system (Chimera Grid System) will be developed and applied to investigate wave-structure interaction. In the proposed numerical model, the unsteady, 3-D spatial averaged Navier-Stokes equations are solved to simulate characteristics of viscous flow fields. And turbulence effects are modeled by using the large eddy simulation (LES). The accuracy of the proposed numerical wave model was verified by comparing the numerical results with experimental data and another numerical results (Mo's thesis, 2010). Having verified the accuracy of the proposed numerical wave model, the model will be developed and continuously improved to investigate the interaction of water waves with 3-D offshore structures.

KEY WORDS: level set method; Chimera grid system; large-eddy simulation; solitary wave

INTRODUCTION

The coastal zone has been recognized as a natural resource for the activities of human beings in many countries. The nearshore has been utilized for various purposes, such as harvesting, transportation, and recreation. In order to safeguard these diverse activities, numerous engineering efforts have been employed in the coastal zone. The mechanism of beach processes has also received the attention of coastal engineers. In coastal areas, artificial structures were very often used to protect harbors, inlets and beaches from wave action. However, shoreline protection should make use of near-nature working methods as opposed to hard (structured) methods. In order to arrive at appropriate engineering methods for shoreline protection, we study the interaction between waves and structures.

There are a wide variety of methods for investigating the interactions occurring between waves and structures. In the past, some previous studies have traditionally investigated the interaction of waves and structures by means of physical model tests (Synolakis, 1986; Hsiao et al., 2008, among many others). In recent years, a great effort has been made to improve numerical models in order to study the interaction between waves and structures. Among existing approaches, two-dimensional Reynolds-Averaged Navier-Stokes (RANS) models (Lin and Liu, 1998 a&b; Guanche et al., 2009; Losada et al., 2008) have revealed that structural functionally and stability can be studied with a high degree of accuracy. Volume-Averaged Reynolds-Averaged Navier-Stokes equations (VARANS), first presented by Hsu et al. (2002), have been solved to characterize wave-induced flows within porous structures. The VARANS equations are adopted in the present study.

To investigate the interaction between irregularly shaped structures and fluid, conventional numerical approaches transform the governing equations and boundary conditions into the body-fitted coordinate system with either a structured grid (Huang et al., 2002 ; Huang et al., 2011), or an unstructured grid (Zienkiewicz et al., 2005).

This study will apply an innovative method (Huang et al., 2015) for simulating the interaction of the flow with stationary structures of irregular shapes based on Cartesian grids. Rather than adding explicitly a forcing term to the momentum equations, this method introduces two boundary velocities to satisfy the zero-velocity (no-slip) boundary condition and the conservation of mass around a stationary immersed solid boundary. The conservation of mass was guaranteed without using the cut-cell method, and the proposed model does not violate mass conservation, as occurs in the conventional immersed boundary method (Kim et al., 2001).

However, simply using the non-uniform Cartesian grid is not often feasible since many simulations require the resolution of details on many different scales. Because the cost of computer memory and the efficiency of computation are also crucial in the numerical computation, this study will solve the governing equations based on an overlapped multi-layer Cartesian grid system, the cell size in each grid net is chosen independently to meet the adaptability. This grid system is often referred to as a "Chimera Grid" (English et al., 2013). Chimera grid embedding uses a number of overlapping grids which are arbitrarily oriented and even of multiple types in order to decompose the domain into regions of interest.

Wave interaction with coastal structures is, in essence, mainly a three-dimensional problem. The most relevant hydraulic processes to be considered in wave–structure interaction encompass wave reflection, wave dissipation, wave transmission resulting from wave overtopping and wave penetration through porous structures, wave diffraction, run-up, and wave breaking. Although, a two-dimensional numerical wave model was developed in recent years, a correct assessment of flow characteristics and the consequent functional response of the structure needs to be performed by taking its three-dimensionality into account.

In the present study, a three-dimensional numerical wave tank in viscous fluid will be developed and applied to simulate the internal velocity and its corresponding surface evolution as the water waves propagation over a permeable structures. The unsteady, 3-D spatial averaged Navier-Stokes equations are solved to simulate characteristics of viscous flow fields. And turbulence effects are modeled by using the large eddy simulation (LES).

MUMERICAL MODEL

In present numerical model, the unsteady, 3-D spatial averaged Navier-Stokes equations are solved to simulate characteristics of viscous flow fields. And turbulence effects are molded by a subgrid-scale (SGS) model using the concept of large eddy simulation (LES). A spatial filter is applied to the Navier-Stokes equations (Lin and Li, 2002):

$$\frac{\partial \overline{u}_i}{\partial x_i} = 0 \tag{1}$$

$$\frac{\partial \overline{u}_i}{\partial t} + \overline{u}_j \frac{\partial \overline{u}_i}{\partial x_j} = -\frac{1}{\rho}\frac{\partial \overline{p}}{\partial x_i} + \frac{\partial}{\partial x_j}(\tau_{ij} + R_{ij}) \tag{2}$$

where $\overline{u}_i$ is the mean velocity in the *ith* component, ρ the fluid density, $\overline{p}$ the mean dynamic pressure, $\tau_{ij} = 2\mu S_{ij}$ the viscous stress, and R_{ij} the stress induced by the filtering process for spatial flow variation. In the above definition, μ is the molecular viscosity and $S_{ij} = (\partial \overline{u}_i / \partial x_j + \partial \overline{u}_j / \partial x_i)/2$ is the rate of strain of the mean flow. In this study, the Smagorinsky model (Smagorinsky, 1963) will be employed. The Smagorinsky model employed in this study treats two parts as a whole

$$R_{ij} = 2\nu_t S_{ij} = 2(L_S^2 \sqrt{S_{ij}S_{ij}})S_{ij} \tag{3}$$

where $\nu_t = L_S^2 \sqrt{S_{ij}S_{ij}}$ is the kinematic molecular viscosity and L_S is the characteristic length scale which equals $C_s(\Delta x \Delta y \Delta z)^{1/3}$ with $C_s = 0.15$.

The governing equations are discretized by means of finite-analytical method. The fractional step technique is adopted for solving the coupling of velocity and pressure. The level set method is used to represent the irregular solid boundary, which can be uneven seabed or multi-slope seawall. The hybrid particle level set method is applied to capture the complex interface between the air and water phases. An innovative solid-fluid coupling method, developed by the principal investigator of this project, is employed to mimic the solid-fluid interaction on fixed Cartesian grids (Huang et al., 2015).

Additionally, our research team simulated the interaction between flow and irregularly shaped structures and got fairly good verification of the two-dimensional numerical wave model. Therefore, in this study, a three-dimensional wave model based on Chimera grid system (English et al., 2013) is developed combined with fluid- solid coupling (Huang et al., 2015). Then, figure 1 shows the Chimera grid system.

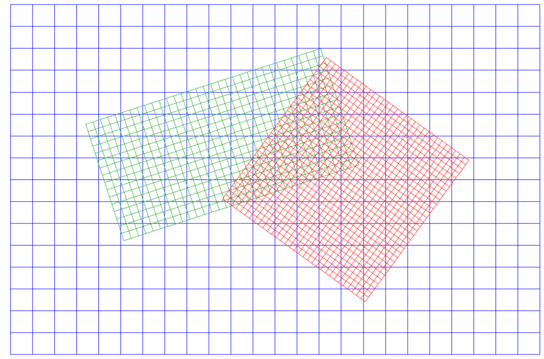

Fig. 1 Schematic of the Chimera grid system. (English et al., 2013)

VALIDATION OF THE MODEL

3D lid-driven cavity flows

A simplified 3-D numerical tank was developed to simulate the lid driven cavity flow in a cubic box. And the numerical results were compared to the results of Žunič et al. (2006). In the computational, the edge length of the cubic cavity is $L = 1$. The Reynolds number is based on the cavity's edge size and the top lid velocity and was selected to be Re = 100. The lid of the cubic cavity moves parallel to the positive x-axis with the velocity u = 1. The quantitative evaluation of the numerical results was shown in figure 2, where we compare v_x and v_z velocity along the centerline.

As mention above, the study will solve the governing equations based on a multi-block Cartesian grid system in present numerical model. In this section, we will study the difference between one-block grid system and two-block grid system. Figure 2 (a) and (b) show the results of the one-block grid system (35*35*35 elements) and the two-block grid system (the whole: 70*70*70 elements, the middle: 20*20*20 elements ($0.25 \leq X, Y, Z \leq 0.75$)), respectively. Figure 2 shows that present 3-D numerical results agree very well with the results of Yang et al. (1998) and Žunič et al. (2006). From figure (b), we could see that the numerical results are much closer to the results of present study around the boundary. Therefore, the numerical model based on a multi-block Cartesian grid system was presented and could get a good agreements between other numerical results.

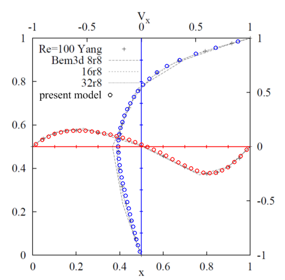

(a)

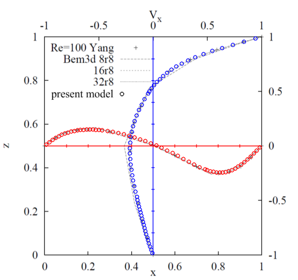

(b)

Fig. 2 Velocity profiles along centerlines for *Re* = 100. (a) one-block grid system (35*35*35 elements); (b) two-block grid system (the whole: 70*70*70 elements, the middle: 20*20*20 elements). (+) results of Yang et al. (1998); (-) results of Žunič et al. (2006); and (o) results of present numerical model.

Solitary wave propagating over a vertical circular cylinder

To check the capability and accuracy of present numerical model, we compare numerical results with another numerical results and experimental data (Mo's thesis, 2010). The experiments were conducted in the Tsunami Wave Basin at the O. H. Hinsdale Wave Research Laboratory (WRL) of the Oregon State University (OSU). The wave basin at the WRL of OSU has an effective length of 160 *ft* (48.8 m), a width of 87 *ft* (26.5 m) and a depth of 7 ft (2.1m). Stainless steel circular cylinders with a diameter, *D*, of 4 *ft* (1.219m) were installed in the basin.

To reduce the computational time, it is designed to use only half width of the wave flume in the numerical simulation. And, the wave gauges were deployed to measure the free surface elevation of solitary wave propagating over a circular cylinder in the numerical wave flume. Figure 3 shows the wave gauges locations. The lateral domain width is 3D for this case to ensure that the reflection from the lateral wall has not reached the cylinders at the end of the numerical simulation.

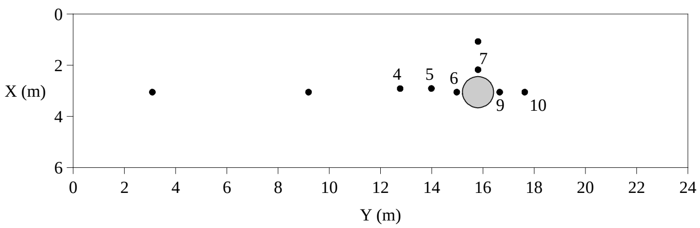

Fig. 3 Sketch of the locations of the cylinder and the wave gauges.

In this numerical simulation, a solitary wave was used for the experimental validation. The incident wave information, including the velocity and the surface displacement, were provided by Grimshaw's 3rd-order solitary wave formula (Grimshaw, 1971) as described in appendixes. For this case that the incident solitary waves with still water depth $h = 0.75$ m and the wave height of the solitary wave $H = 0.3$ m propagate over a circular cylinder.

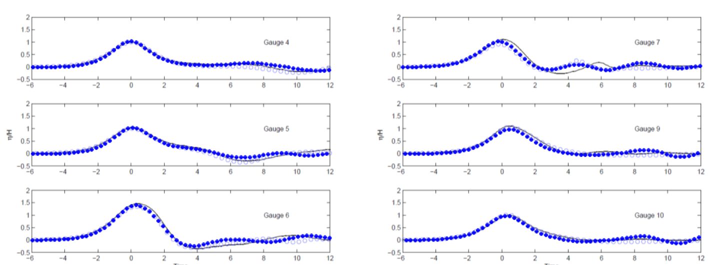

Fig. 4 Time history of free surface elevations at wave gauges for this simulation case. (◦) experimental data (Mo's thesis, 2010); (-) the results of another numerical model (Mo's) thesis; (•) the results of present numerical model.

The numerical results of the time histories of free surface elevations at 6 wave gauges locations (see figure 3) are shown in figure 4. Figure 4 shows that present numerical results agree well with another numerical results and the experimental data (Mo's thesis, 2010). Figure 4 also shows that as the solitary wave propagates to the cylinder, its wave height gets higher due to the blockage of the cylinder. In figure 4's Gauge 4 ~ 7, we can see a noticeable scattering wave from the cylinder. The first scattered wave is due to the wave reflection from the front side of the cylinder. The secondary scattered wave was caused by a relative higher surface displacement at the lee side of the cylinder. However, the present numerical results does not match

CONCLUSIONS

In this study, a three-dimensional (3-D) numerical wave model based on a Chimera Grid System will be developed to solve 3-D wave-structure interaction problem. And the proposed numerical model has been tested some cases with other's numerical results and experimental data. The good comparisons show that out numerical model is capable of predicting fluid velocity and free surface displacement. Besides, the wave dynamic pressure and the wave force acting on a structure play an important role in the costal engineering. Then, the present numerical wave model will be modified and applied for simulating the aforementioned case. And the proposed numerical model results will be verified with the experimental data or another numerical model results.

After the accuracy of the proposed numerical wave model is verified, the effects of several parameters on the interaction between waves and structures will be investigated and calibrated. One of the benefits of using the multi-block grid system for simulating the wave-structure interactions is that the boundary layer flows induced by water waves at a slope can be determined, which has not been done in the literature. Finally, we believe that this proposed study will lead to the better understanding of the interaction between wave and structures, and the mechanism of flow field in boundary layer on sloping sea bed or seawall, especially.

ACKNOWLEDGEMENTS

This research was financially supported by the Ministry of Science and Technology, R.O.C., under grant MOST 104-2221-E-006-183.

REFERENCES

English, R.E., Qiu, L., Yu, Y., and Fedkiw, R. (2013). An adaptive discretization of incompressible flow using a multitude of moving Cartesian grids. J. Comput. Phys., Vol. 254, pp. 107-154.

Grimshaw, R. (1971). The solitary wave in water of variable depth. J. Fluid Mech., 46(2):611-622, 1971.

Guanche, R., Losada, I.J., Lara, J.L. (2009). Numerical analysis of wave loads for coastal structure stability. Coastal Eng. 56 (5-6), 543-558.

Hsiao, S.C., Hsu, T.W., Lin, T.C., and Chang, Y.H. (2008). On the evolution and run-up of breaking solitary waves on a mild sloping beach. Coastal Eng., Vol. 55, pp. 975-988.

Hsu, T.J., Sakakiyama, T., Liu, P.L.–F. (2002), A numerical model for wave motions and turbulence flows in front of a composite breakwater. Coastal Eng., Vol. 46, pp. 25-50.

Huang C.J., Dong C.M. (2002). Propagation of water waves over rigid rippled beds. J WATERW PORT COAST OCEAN ENG ASCE 2002; 128:190-201.

Huang C.J., Lin, C.Y., and Chen C.H. (2015). Numerical simulations of fluid-structure interaction based on Cartesian grids with two boundary velocities. Int. J. Num. Methods Fluids, Vol. 79, No. 3, pp. 138-161.

Huang, C.J., Chen, C.H., Chang, H.H. (2011). Propagation of water waves over permeable rippled beds, Ocean Engineering 2011; 38:579-591.

Kim, J., Kim, D., and Choi, H. (2001). An immersed-boundary finite-volume method for simulations of flow in complex geometries. J. Comput. Phys., Vol. 171, pp. 132-150.

Lin, P. and Li. C.W. (2002). Wave-current interaction with a vertical square cylinder. Ocean Engineering 2003, pp. 855 – 876.

Lin, P. and Liu, P.L.F. (1998a). A numerical study of breaking waves in the surf zone. J. Fluid Mech., Vol. 359, pp. 239-264.

Lin, P. and Liu, P.L.F. (1998b). Turbulence transport, vorticity dynamics, and solute mixing under plunging breaking waves in surf zone. J. Geophys. Res., Vol. 103(C8), pp. 15677-15694.

Losada, I.J., Lara, J.L., Guanche, R., Gonzalez Ondina, J. (2008). Numerical analysis of wave overtopping of rubble mound breakwaters. Coastal Eng. 55 (1), 47-62.

Mo, W.H. (2010) Numerical investigation of solitary wave interaction with group of cylinders. PhD Thesis, Cornell University.

Smagorinsky, J. (1963). General circulation experiments with primitive equations. Mon. Weather Rev., Vol. 91, No. 3, pp. 99-164.

Synolakis, C.E. (1986). The runup of long waves. Ph.D. Thesis, California Institute of Technology, Pasadena, California.

Yang, J.Y.; Yang, S.C.; Chen, Y.N.; Hsu, C.A. (1998). Implicit weighted ENO schemes for the three-dimensional incompressible Navier-Stokes equations. J. Comput. Phys., Vol. 146, pp. 464-487.

Zienkiewicz O.C., Taylor R.L. (2005). Nithiarasu, P. The Finite Element Method for Fluid Dynamics, 6th Ed., Elsevier.

Žunič, Z., Hribersek, M., Skerget, L., and Ravnik, J. (2006). 3D lid driven cavity flow by mixed boundary and finite element method. European Conference on Computational Fluid Dynamics. ECCOMAS CFD 2006, pp. 1-12.

APPENDIXES

In the proposed numerical simulation, the free surface displacement and velocity distribution on the incident boundary are calculated by 3rd-order Grimshaw solitary wave solution:

$$\eta == h\left[\left(\frac{H}{h}\right)S^2 - \frac{3}{4}\left(\frac{H}{h}\right)^2 S^2T^2 + \left(\frac{H}{h}\right)^3\left(\frac{5}{8}S^2T^2 - \frac{101}{80}S^4T^2\right)\right]$$

where H is the wave height; h is the still water depth; $S = \operatorname{sec}h\,\alpha X/h$; $T = \tanh \alpha X/h$; $X = x - Ct$ in which C is the wave speed; the coefficient α :

$$\alpha = \left(\frac{3}{4}\frac{H}{h}\right)^{1/2}\left(1 - \frac{5}{8}\frac{H}{h} + \frac{71}{128}\frac{H^2}{h^2}\right)$$

and the wave speed C is:

$$C = \sqrt{gh}\left(1 + \frac{H}{h} - \frac{1}{20}\frac{H^2}{h^2} - \frac{3}{70}\frac{H^3}{h^3}\right)$$

and the velocity distribution is:

$$\begin{aligned}\frac{v}{\sqrt{gh}} = &\left(\frac{H}{h}\right)S^2 - S^2\left(\frac{H}{h}\right)^2\left[-\frac{1}{4} + S^2 + \left(\frac{z}{h}\right)^2\left(\frac{3}{2} - \frac{9}{4}S^2\right)\right] \\ &- S^2\left(\frac{H}{h}\right)^3\left[\frac{19}{40} + \frac{1}{5}S^2 - \frac{6}{5}S^4\right. \\ &+ \left(\frac{z}{h}\right)^2\left(-\frac{3}{2} - \frac{15}{4}S^2 + \frac{15}{2}S^4\right) \\ &\left.+ \left(\frac{z}{h}\right)^4\left(-\frac{3}{8} + \frac{45}{16}S^2 - \frac{45}{16}S^4\right)\right]\end{aligned}$$

$$\begin{aligned}\frac{w}{\sqrt{gh}} = &\sqrt{3\left(\frac{H}{h}\right)}\left(\frac{z}{h}\right)S^2T\left\{-\left(\frac{H}{h}\right) + \left(\frac{H}{h}\right)^2\left[\frac{3}{8} + 2S^2 + \left(\frac{z}{h}\right)^2\left(\frac{1}{2} - \frac{3}{2}S^2\right)\right]\right. \\ &+ \left(\frac{H}{h}\right)^3\left[\frac{49}{640} - \frac{17}{20}S^2 - \frac{18}{5}S^4 + \left(\frac{z}{h}\right)^2\left(-\frac{13}{16} - \frac{25}{16}S^2 + \frac{15}{2}S^4\right)\right. \\ &\left.\left.+ \left(\frac{z}{h}\right)^4\left(-\frac{3}{40} + \frac{9}{8}S^2 - \frac{27}{16}S^4\right)\right]\right\}\end{aligned}$$